Excitation-Photon-Energy Selectivity of Photoconversions in Halogen-Bridged Pd-Chain Compounds: Mott Insulator to Metal or Charge-Density-Wave State

H. Matsuzaki,[1,*] M. Iwata,[1] T. Miyamoto,[1] T. Terashige,[1] K. Iwano,[2] S. Takaishi,[3] M. Takamura,[3] S. Kumagai,[3] M. Yamashita,[3] R. Takahashi,[4] Y. Wakabayashi,[4] and H. Okamoto[1]

[1]*Department of Advanced Materials Science, University of Tokyo, Kashiwa, Chiba 277-8561, Japan*
[2]*Institute of Materials Structure Science, Graduate University for Advanced Studies, High Energy Accelerator Research Organization (KEK), Tsukuba 305-0801, Japan*
[3]*Department of Chemistry, Tohoku University, Sendai, Miyagi 980-8578, Japan*
[4]*Division of Materials Physics, Graduate School of Engineering Science, Osaka University, Toyonaka 560-8531, Japan*

(Received 9 December 2013; revised manuscript received 30 June 2014; published 28 August 2014)

Ultrafast photoinduced transitions of a one-dimensional Mott insulator into two distinct electronic phases, metal and charge-density-wave (CDW) state, were achieved in a bromine-bridged Pd-chain compound $[Pd(en)_2Br](C_5\text{-}Y)_2H_2O$ (en = ethylenediamine and C_5-Y = dialkylsulfosuccinate), by selecting the photon energy of a femtosecond excitation pulse. For the resonant excitation of the Mott-gap transition, excitonic states are generated and converted to one-dimensional CDW domains. For the higher-energy excitation, free electron and hole carriers are produced, giving rise to a transition of the Mott insulator to a metal. Such selectivity in photoconversions by the choice of initial photoexcited states opens a new possibility for the developments of advanced optical switching and memory functions.

DOI: 10.1103/PhysRevLett.113.096403 PACS numbers: 71.30.+h, 71.45.Lr, 78.40.Ha, 78.47.J–

Ultrafast changes of electronic states in solids by light, called photoinduced phase transitions (PIPTs), are recently attracting considerable attention as new mechanisms for future optical switching and memory devices [1,2]. A key strategy for realizing a PIPT is to photoexcite a material located near a boundary between two different electronic phases. Following this strategy, several PIPTs between two nearly degenerate phases have been reported so far, e.g., the neutral-ionic transition in tetrathiafulvalene-*p*-chloranil [3–7], the insulator-metal transition in VO_2 [8–12], and the charge- or orbital-order insulator to ferromagnetic metal transition in manganites [13–19]. In some of these PIPTs, transition behaviors were investigated using different excitation photon energies, and it was observed that they affected the transition efficiency [5,15,20,21] and transition time [22]. A more exotic method of photocontrol is to generate two different phases by the choice of the excitation photon energy. This can provide a good opportunity for the exploration of new optical switching and memory devices, as well as for advanced studies of PIPTs. However, such selectivity in PIPTs has hardly been achieved [23]. In the present study, we show that by a choice of the photon energy of a femtosecond laser pulse, a quasi-one-dimensional (1D) Mott insulator can be changed either to a metal or a charge-density-wave (CDW) insulator.

The material studied is a bromine-bridged Pd-chain compound $[Pd(en)_2Br](C_5\text{-}Y)_2H_2O$ (en = ethylenediamine, C_5-Y = dialkylsulfosuccinate) [Fig. 1(a)] [24], which is one of the halogen (*X*)-bridged transition-metal (*M*) compounds (*MX* chains). In *MX* chains, *M* (Ni, Pd, Pt) ions and *X* (Cl, Br, I) ions arrange alternately and the 1D electronic state is formed by the p_z orbital of *X* and the d_z^2 orbital of *M* [25]. *MX* chains have two stable electronic phases, the Mott-insulator phase ($\ldots X^-\text{-}M^{3+}\text{-}X^-\text{-}M^{3+}\text{-}X^-\ldots$) in which M^{3+} ions and X^- ions are regularly arranged, and the CDW phase ($\ldots X^-\text{-}M^{4+}\text{-}X^-\text{--}M^{2+}\text{--}X^-\text{-}M^{4+}\text{-}X^-\text{--}M^{2+}\text{--}X^-\ldots$) in which M^{2+} and M^{4+} are alternately arranged with dimeric displacements of X^- ions [26]. $[Pd(en)_2Br](C_5\text{-}Y)_2H_2O$ is a unique material that shows a CDW to Mott-insulator transition [24]. With lowering temperature, the neighboring Pd-Pd distance (*L*) along the chain axis **b** [open circles in Fig. 1(b)] gradually decreases because of the suppression of thermal motions of the alkyl chains, leading to the enhancement of their packing through van der Waals attractions. At $T_c = 205$ K, this compound undergoes a first-order transition from CDW to Mott-insulator via a discontinuous change of the optical-gap energy E_g as well as *L* [Fig. 1(b)] [24,27]. Suppression of the electron-lattice interaction associated with the bridging Br ions due to the decrease in *L* [28] is a main driving force for this transition. Hereafter, we abbreviate $[Pd(en)_2Br](C_5\text{-}Y)_2H_2O$ as PdBrC5 [24].

Below T_c, two kinds of PIPTs can be expected in PdBrC5. One is the photoinduced Mott-insulator to metal transition [Fig. 1(c)], which was previously observed in another 1D Mott insulator $[Ni(chxn)_2Br]Br_2$ (chxn = cyclohexanediamine) [29], and a 1D organic Mott insulator, bis(ethylenedithio)tetrathiafulvalene-difluorotetracyanoquinodimethane (ET-F_2TCNQ) [30,31]. In those transitions, photogenerated electron and hole carriers act as free carriers because of the nature of the spin-charge separation characteristic of 1D correlated electron systems [32,33]. The other possible PIPT is the

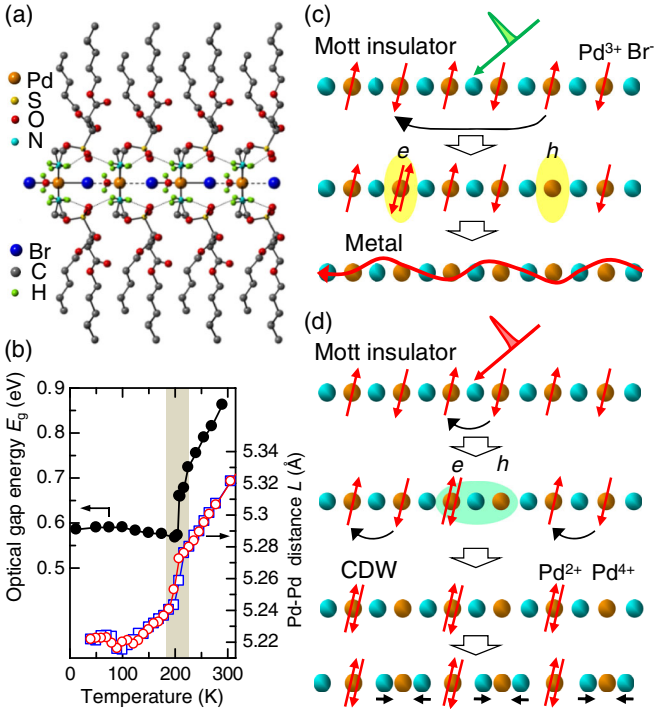

FIG. 1 (color online). (a) Crystal structure of $[Pd(en)_2Br](C_5\text{-}Y)_2H_2O$. H atoms of C_5-Y are omitted for clarity. (b) Temperature dependence of the optical-gap energy E_g and the Pd-Pd distance L (open circles: cooling run, open squares: heating run) [24]. Schematics of (c) photoinduced Mott-insulator to metal transition and (d) photoinduced Mott-insulator to CDW transition.

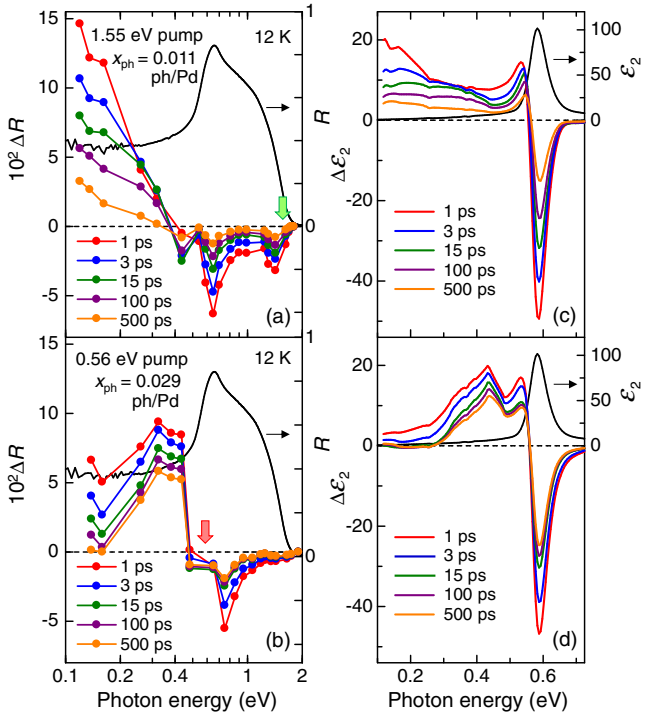

FIG. 2 (color online). (a),(b) Reflectivity (R) spectrum (thick solid lines) and its photoinduced changes (ΔR) of $[Pd(en)_2Br](C_5\text{-}Y)_2H_2O$ at 12 K; (a) 1.55 eV pump and (b) 0.56 eV pump. Arrows indicate pump energies. (c),(d) Spectrum of the imaginary part of the dielectric constant (ε_2) (thick solid lines) and its photoinduced changes ($\Delta\varepsilon_2$) at 12 K; (c) 1.55 eV pump and (d) 0.56 eV pump. Pump and probe lights are $\|$ **b**.

photoinduced Mott-insulator to CDW transition [Fig. 1(d)], since Mott-insulator and CDW phases are nearly degenerate in PdBrC5. We show that this transition can be driven via the creation of a Pd^{4+}-Pd^{2+} pair as the precursor state of CDW by a resonant excitation of the lowest excitonic state.

Single crystals of PdBrC5 were prepared following a previous report [24]. For pump-probe measurements, a $Ti:Al_2O_3$ regenerative amplifier (RA) was used as a light source (1.55 eV, pulse width of 130 fs, and repetition rate of 1 kHz). The output from the RA was divided into two pulses, which were used as excitation sources for two optical parametric amplifiers (OPAs). From two OPAs, pump (0.56 eV) and probe (0.1–2 eV) pulses were obtained. For the 1.55 eV pump, the output from the RA was directly used. The delay time t_d of the probe pulse relative to the pump pulse was controlled by changing the path length of the pump pulse. The temporal resolution of the system was ~180 fs. Polarized Raman spectra were measured using a Raman spectrometer equipped with a He-Ne laser and an optical microscope.

In Figs. 2(a) and 2(b), we show using solid lines the polarized reflectivity (R) spectra of PdBrC5 at 12 K with the light electric field E parallel ($\|$) to the chain axis **b**. The imaginary part of the dielectric constant ε_2 [solid lines in Figs. 2(c) and 2(d)] was obtained by using the Kramers-Kronig transformation (KKT) of the R spectra [34]. The ε_2 spectrum exhibits a sharp peak at 0.585 eV corresponding to the Mott-gap transition. More strictly, this peak is attributed to a 1D exciton, expressed as $(Pd^{3+}, Pd^{3+}) \rightarrow (Pd^{2+}, Pd^{4+})$, since the excitonic effect is effective in most of the MX chains [28,35]. Hereafter, we call this exciton the Mott-gap exciton.

In Fig. 2(a), the spectra of photoinduced reflectivity changes (ΔR) using the 1.55 eV pump are presented for typical delay times t_d. Electric fields of the pump and probe lights are $\|$ **b**. The averaged photon density (x_{ph}) of a pump pulse absorbed within the absorption depth (1210 Å) is 0.011 photon (ph)/Pd [36]. The evaluation procedures of x_{ph} are detailed in the Supplemental Material S1 [37]. R in the mid-IR region below 0.4 eV shows noticeable increase with decrease in energy for each t_d value in common, being reminiscent of a Drude response, while R decreases over a wide energy region (0.4–2 eV) showing spectral weight transfer to the IR region. To get more detailed information on the transient electronic-state changes, we calculated the photoinduced change, $\Delta\varepsilon_2$, by KKT of the $R + \Delta R$ spectra [colored lines in Fig. 2(c)] [43]. The spectral intensity of $\Delta\varepsilon_2$ at $t_d = 1$ ps monotonically increases with decreasing energy, suggesting the formation of a metallic state. Such a spectral feature is almost unchanged up to 500 ps.

To achieve the photoinduced Mott-insulator to CDW transition, we next set the pump photon energy at 0.56 eV corresponding to the Mott-gap exciton. ΔR and $\Delta\varepsilon_2$ spectra for $t_d = 1$–500 ps ($x_{\rm ph} = 0.029$ ph/Pd), shown in Figs. 2(b) and 2(d), respectively, are considerably different from those collected using the 1.55 eV pump [Figs. 2(a) and 2(c)]. $\Delta\varepsilon_2$ spectra have small intensities below 0.2 eV and exhibit a clear peak structure at around 0.4 eV. We ascertained that time profiles of ΔR for the 1.55 and 0.56 eV pump are much different even at the same excitation-photon-density ($x_{\rm ph}$). This demonstrates that different photoresponses of the 1.55 and 0.56 eV pump (Fig. 2) are not due to the difference in $x_{\rm ph}$(= 0.011 and 0.029 ph/Pd). The $x_{\rm ph}$ dependences of ΔR for the 1.55 and 0.56 eV pump and ΔR spectra for $t_d < 1$ ps are presented in the Supplemental Material S2 [37].

To characterize the observed photoinduced states, we analyzed the ε_2 spectra at $t_d = 1$ ps in Figs. 3(a) and 3(b). We assume that these spectra consist of two components, the original Mott-gap-exciton transition with a Lorentzian spectral shape (blue area) and the other component originating from the photoinduced state (green or red areas). The details of the analyses are reported in the Supplemental Material S3 [37]. For the 1.55 eV pump, the blue area depicts the reduced Mott-gap-exciton transition with a peak at 0.57 eV and the green area depicts metallic behavior. In contrast, for the 0.56 eV pump, the spectrum was well reproduced by the sum (the solid line) of two Lorentzian components with peaks at 0.57 eV (blue area) and 0.41 eV (red area). This suggests that a metastable state, characterized by the 0.41 eV peak, is photogenerated. The CDW state is a plausible candidate for this metastable state.

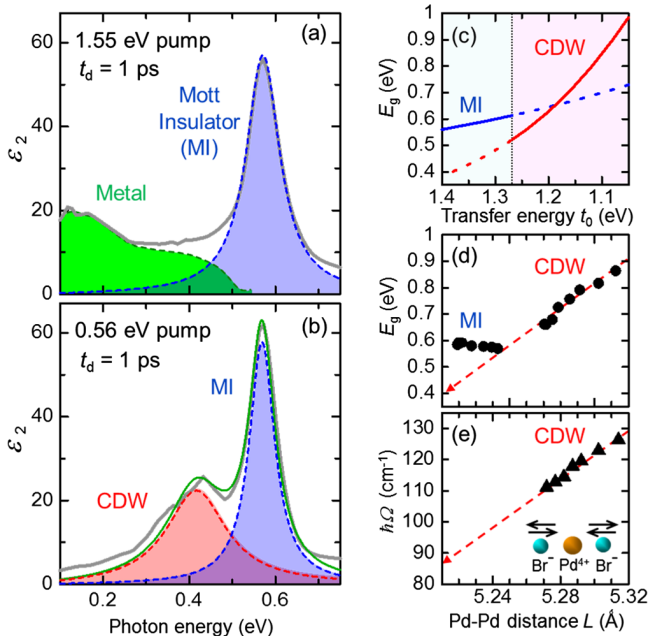

FIG. 3 (color online). (a),(b) ε_2 spectra along **b** at 12 K and at $t_d = 1$ ps in $[Pd(en)_2Br](C_5\text{-}Y)_2H_2O$; (a) 1.55 eV pump and (b) 0.56 eV pump (thick solid lines). Blue shaded areas show the responses of the Mott-insulator state. Green shaded area in (a) shows the response of the photoinduced metallic state. Red shaded area in (b) shows the response of the photoinduced CDW state. Thin solid line is the fitting curve. (c) Calculated E_g as a function of the transfer energy t_0. (d) Optical-gap energy E_g and (e) frequency $\hbar\Omega$ of the symmetric Pd-Br stretching mode as a function of the Pd-Pd distance L.

The peak energy (0.41 eV) of the photoinduced state using the 0.56 eV pump is, however, smaller than that of the CDW state (>0.66 eV) for $T > T_c = 205$ K [Fig. 1(b)]. We can attribute this difference to the temperature dependence of the Pd-Pd distance, L. Figure 3(d) shows the optical-gap energy E_g corresponding to the CDW-gap exciton as a function of L, which was deduced from Fig. 1(b). With a decrease in L, E_g linearly decreases in the CDW phase. Such a linear relation is well known in MX chains with CDW and is explained by the extended-Peierls-Hubbard model [28]. Taking the L value (~5.22 Å) at 12 K into account, E_g of the photoinduced CDW state is expected to be close to 0.4 eV [see the broken line in Fig. 3(d)].

To confirm this interpretation, it is important to demonstrate that the variation of E_g across the CDW and Mott-insulator boundary can be explained by reasonable changes in physical parameters due to the decrease in L. For this purpose, we adopted the extended-Peierls-Hubbard model with physical parameters, the on-site Coulomb repulsion U, the intersite Coulomb repulsion V, the electron-lattice interaction S, and transfer energy t_0. The Hamiltonian is given by

$$H = -t_0\sum_{l,\sigma}(C^+_{l+1\sigma}C_{l\sigma} + \text{H.c.}) + U\sum_l n_{l\uparrow}n_{l\downarrow} + V\sum_l n_l n_{l+1} - S\sum_l (q_{l+1} - q_l)n_l + \frac{S}{2}\sum_l q_l^2, \quad (1)$$

where $C_{l\sigma}(C^+_{l\sigma})$ is the operator for $4d_{z^2}$ electrons with spin σ at the lth Pd site, n_l is its number operator, and q_l is a dimensionless displacement of the lth Br ions from the midpoints between the neighboring two Pd ions. S is expressed as α^2/K, where α is the original electron-lattice interaction coefficient and K is the elastic constant. In order to reproduce the L dependence of E_g, we calculated the gap energies by adjusting U, V, S, and t_0 in the framework of the 16-site exact diagonalization and the optimization of the displacements of Br ions [44,45]. In this procedure, we assumed that with a decrease in L, t_0 increases from 1 to 1.4 eV and S rather decreases from 0.275 to 0.255 eV as $S = 0.275 - (t_0 - 1)\times 0.05$ in units of eV [46] because of the hardening of the elasticity. With $U = 3.4$, $V = 1.35$, and $t_0 = 1.05$–1.4 eV, we obtained the gap energies of the two states as a function of t_0 and the phase boundary as shown in Fig. 3(c), which are fairly consistent with the result in Fig. 3(d).

In order to further check the validity of those theoretical analyses, we calculated the t_0 dependence of the frequency $\hbar\Omega$ of the symmetric Pd-Br stretching mode illustrated in the inset of Fig. 3(e), since the L dependence of $\hbar\Omega$ was obtained by the previous Raman studies [Fig. 3(e)]. The calculation results could reproduce the important features of the experimental results; the frequency ($\sim$130 cm^{-1}) at room temperature decreases by about 15% near the phase boundary ($\sim$110 cm^{-1}). The decrease in the frequency is caused by the reduction in the bridging-Br displacements, which overcomes the effect of the hardening of the elasticity. The details of the Raman-mode frequency calculation are reported in the Supplemental Material S4 [37].

Next, we discuss the dynamics of the observed PIPTs. In Fig. 4(a), we show the time profiles of $\Delta R/R$ at 0.16 eV for the 1.55 eV pump and at 0.32 eV for the 0.56 eV pump at the same $x_{\rm ph}$ value (0.0066 ph/Pd), which reflect the dynamics of the photoinduced metal and CDW states, respectively. From $\Delta R/R$ for the 1.55 eV pump, we can see

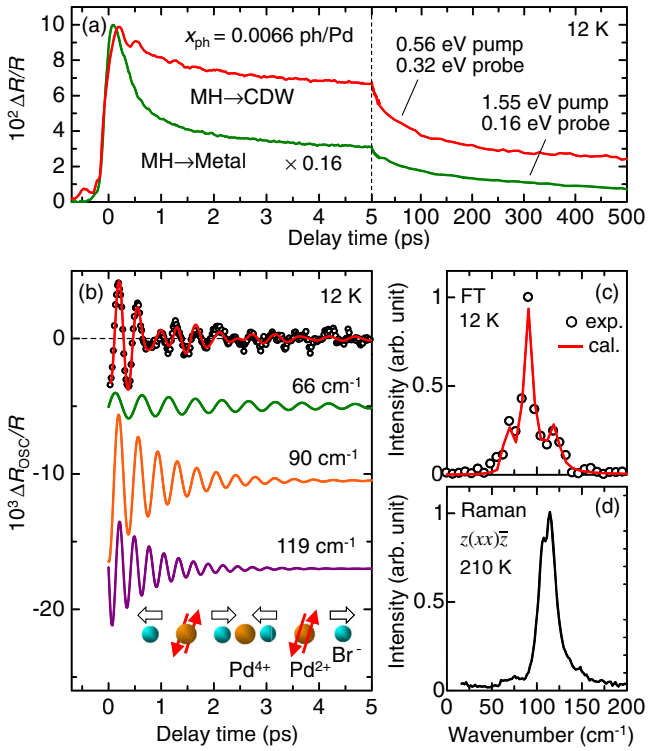

FIG. 4 (color online). (a) Time profiles of $\Delta R/R$ at 12 K in $[Pd(en)_2Br](C_5\text{-}Y)_2H_2O$ for $x_{\rm ph} = 0.0066$ ph/Pd. (b) Oscillatory component $\Delta R_{\rm OSC}/R$ (open circles) extracted from $\Delta R/R$ by the 0.56 eV pump and 0.32 eV probe shown in (a). The upper solid line is a fitting curve, which is the sum of the three damped oscillations shown in the lower part. The inset exhibits the symmetric Pd-Br stretching mode responsible for the 90 cm^{-1} oscillation. (c) Fourier power spectrum of the oscillatory component shown in (b) (open circles) and the fitting curve (solid line). (d) Polarized Raman spectrum for the 1.96 eV excitation at 210 K (CDW). x corresponds to the **b** axis and z z is normal to the bc plane.

that the metallic state is formed within the time resolution and its primary decay for $t_d < 1$ ps is very fast. For $t_d > 1$ ps, the metallic state decays with a time constant of $\sim$100 ps. From $\Delta R/R$ for the 0.56 eV pump, we find that the CDW state is also formed within the time resolution. It decays with a time constant of $\sim$500 ps, indicating that the photoinduced CDW state is more stable than the photoinduced metallic state. In the time region up to 5 ps, a coherent oscillation was observed. As shown in Fig. 4(b) (the upper solid line), the time characteristic of the oscillatory component (open circles) was well reproduced by assuming three damped oscillators (the lower three solid lines). The details of the analyses are reported in the Supplemental Material S5 [37]. We show in Fig. 4(c) the Fourier power spectra of the oscillatory component (open circles) and its fitting curve (the red line), which are in good agreement with each other. The main oscillation with 90 cm^{-1} is of a cosine-type, which is attributed to the coherent oscillation driven by a displacive-excitation mechanism [47]. Since the CDW states accompany the bridging-Br displacements, it is reasonable to assign this 90 cm^{-1} oscillation to the symmetric Pd-Br stretching mode in the photogenerated CDW domains [see the inset of Fig. 4(b)]. In fact, the spectral shape of the Fourier power spectrum [Fig. 4(c)] is very similar to that of the corresponding Raman band at 210 K [Fig. 4(d)]. However, the peak is located at 110 cm^{-1}. This discrepancy in the frequency can be understood again by considering the temperature dependence of L. Since the frequency of this mode decreases with a decrease in L [the broken line in Fig. 3(e)] [48], we can consider that the oscillation frequency in CDW domains is decreased from $\sim$110 cm^{-1} ($L\sim$5.27 Å) at 210 K to $\sim$90 cm^{-1} ($L\sim$5.22 Å) at 12 K. The coherent oscillation due to the symmetric Pd-Br stretching mode itself is strong evidence for the occurrence of the Mott-insulator to CDW transition.

Finally, we discuss the conversion efficiency Φ of the Mott-insulator to CDW transition. In the case of the resonant excitation [Fig. 3(b)], Φ could be evaluated by the decrease in the integrated spectral weight of the Mott-gap exciton transition. The conversion fraction from Mott insulator to CDW is 34% at $t_d = 1$ ps for $x_{\rm ph} = 0.029$ ph/Pd, giving $\Phi \sim 12$ Pd sites/ph. Such a large Φ is attributed to the close energies of the Mott-insulator and CDW states and also to the collective nature of CDW (see the Supplemental Material S6 [37]).

In summary, we demonstrated that the Mott insulator could be selectively converted to the transient metallic state or CDW state by high-energy excitation and resonant excitation to the Mott-gap exciton, respectively, using femtosecond laser pulses. For the photoinduced Mott-insulator to CDW transition, a large CDW domain ($\sim$12 Pd sites) is formed within the time resolution from an excitonic state and subsequently stabilized by the dimeric Br displacements, accompanied by the coherent Pd-Br

oscillations. The pump-photon-energy-dependent phase transitions presented here will open new possibilities for developing selective controls for optical switching and memory devices.

This work has been partly supported by a Grant-in-Aid for Scientific Research from the Japan Society for the Promotion of Science (No. 22740197) and the Ministry of Education, Culture, Sports, Science, and Technology in Japan (No. 20110005).

*Present address: Research Institute of Instrumentation Frontier, National Institute of Advanced Industrial Science and Technology (AIST), 1-1-1 Umezono, Tsukuba, Ibaraki 305-8568, Japan.

[1] For a review, see *Photoinduced Phase Transitions*, edited by K. Nasu (World Scientific, Singapore, 2004).
[2] S. Iwai and H. Okamoto, J. Phys. Soc. Jpn. **75**, 011007 (2006).
[3] S. Koshihara, Y. Tokura, T. Mitani, G. Saito, and T. Koda, Phys. Rev. B **42**, 6853 (1990).
[4] E. Collet, M. H. Cailleau, M. B. Cointe, H. Cailleau, M. Wulff, T. Luty, S. Koshihara, M. Meyer, L. Toupet, P. Rabiller, and S. Techert, Science **300**, 612 (2003).
[5] H. Okamoto, Y. Ishige, S. Tanaka, H. Kishida, S. Iwai, and Y. Tokura, Phys. Rev. B **70**, 165202 (2004).
[6] S. Iwai, Y. Ishige, S. Tanaka, Y. Okimoto, Y. Tokura, and H. Okamoto, Phys. Rev. Lett. **96**, 057403 (2006).
[7] H. Uemura and H. Okamoto, Phys. Rev. Lett. **105**, 258302 (2010).
[8] A. Cavalleri, Cs. Tóth, C. W. Siders, J. A. Squier, F. Ráksi, P. Forget, and J. C. Kieffer, Phys. Rev. Lett. **87**, 237401 (2001).
[9] A. Cavalleri, M. Rini, H. H. W. Chong, S. Fourmaux, T. E. Glover, P. A. Heimann, J. C. Kieffer, and R. W. Schoenlein, Phys. Rev. Lett. **95**, 067405 (2005).
[10] C. Kübler, H. Ehrke, R. Huber, R. Lopez A. Halabica, R. F. Haglund, Jr., and A. Leitenstorfer, Phys. Rev. Lett. **99**, 116401 (2007).
[11] P. Baum, D.-S. Yang, A. H. Zewail, Science **318**, 788 (2007).
[12] S. Wall, L. Foglia, D. Wegkamp, K. Appavoo, J. Nag, R. F. Haglund, Jr., J. Stähler, and M. Wolf, Phys. Rev. B **87**, 115126 (2013).
[13] M. Fiebig, K. Miyano, Y. Tomioka, and Y. Tokura, Science **280**, 1925 (1998).
[14] M. Fiebig, K. Miyano, Y. Tomioka, and Y. Tokura, Appl. Phys. B **71**, 211 (2000).
[15] M. Rini, R. Tobey, N. Dean, J. Itatani, Y. Tomioka, Y. Tokura, R. W. Schoenlein, and A. Cavalleri, Nature (London) **449**, 72 (2007).
[16] M. Matsubara, Y. Okimoto, T. Ogasawara, Y. Tomioka, H. Okamoto, and Y. Tokura, Phys. Rev. Lett. **99**, 207401 (2007).
[17] Y. Okimoto, H. Matsuzaki, Y. Tomioka, I. Kezsmarki, T. Ogasawara, M. Matsubara, H. Okamoto, and Y. Tokura, J. Phys. Soc. Jpn. **76**, 043702 (2007).
[18] N. Takubo, I. Onishi, K. Takubo, T. Mizokawa, and K. Miyano, Phys. Rev. Lett. **101**, 177403 (2008).
[19] D. Polli, M. Rini, S. Wall, R. W. Schoenlein, Y. Tomioka, Y. Tokura, G. Cerullo, and A. Cavalleri, Nat. Mater. **6**, 643 (2007).
[20] N. Hosaka, H. Tachibana, N. Shiga, M. Matsumoto, and Y. Tokura, Phys. Rev. Lett. **82**, 1672 (1999).
[21] H. Matsuzaki, W. Fujita, K. Awaga, and H. Okamoto, Phys. Rev. Lett. **91**, 017403 (2003).
[22] Y. Kawakami, S. Iwai, T. Fukatsu, M. Miura, N. Yoneyama, T. Sasaki, and N. Kobayashi, Phys. Rev. Lett. **103**, 066403 (2009).
[23] N. O. Moussa, G. Molnár, S. Bonhommeau, A. Zwick, S. Mouri, K. Tanaka, J. A. Real, and A. Bousseksou, Phys. Rev. Lett. **94**, 107205 (2005).
[24] S. Takaishi, M. Takamura, T. Kajiwara, H. Miyasaka, M. Yamashita, M. Iwata, H. Matsuzaki, H. Okamoto, H. Tanaka, S. Kuroda, H. Nishikawa, H. Oshio, K. Kato, and M. Takata, J. Am. Chem. Soc. **130**, 12080 (2008).
[25] M. B. Robin and P. Day, *Advances in Inorganic Chemistry and Radiochemistry*, edited by H. J. Emeleus (Academic Press, New York, 1967), Vol. 10, p. 217.
[26] *Material Designs, and New Physical Properties in MX- and MMX-Chain Compounds*, edited by M. Yamashita and H. Okamoto (Springer, Wien, 2013).
[27] The L values for $T > 110$ K are taken from Ref. [24]. Those for $T < 110$ K were evaluated from the angles of the 020 Bragg reflection.
[28] H. Okamoto and M. Yamashita, Bull. Chem. Soc. Jpn. **71**, 2023 (1998).
[29] S. Iwai, M. Ono, A. Maeda, H. Matsuzaki, H. Kishida, H. Okamoto, and Y. Tokura, Phys. Rev. Lett. **91**, 057401 (2003).
[30] H. Okamoto, H. Matsuzaki, T. Wakabayashi, Y. Takahashi, and T. Hasegawa, Phys. Rev. Lett. **98**, 037401 (2007).
[31] H. Uemura, H. Matsuzaki, Y. Takahashi, T. Hasegawa, and H. Okamoto, J. Phys. Soc. Jpn. **77**, 113714 (2008).
[32] M. Ogata and H. Shiba, Phys. Rev. B **41**, 2326 (1990).
[33] H. Eskes and A. M. Oleś, Phys. Rev. Lett. **73**, 1279 (1994).
[34] The Roessler correction was used in KKT. See, D. M. Roessler, Br. J. Appl. Phys. **16**, 1119 (1965).
[35] M. Ono, K. Miura, A. Maeda, H. Matsuzaki, H. Kishida, Y. Taguchi, Y. Tokura, M. Yamashita, and H. Okamoto, Phys. Rev. B **70**, 085101 (2004).
[36] The excitation photon density x_{ph} was defined by the photon density per unit volume within the absorption depth and evaluated by $x_{\mathrm{ph}} = (1 - 1/e)(1 - R_p)I_p/l_p$, where I_p, l_p, R_p, and e are the excitation photon density per unit area, the absorption depth, the reflection loss of the pump light, and Napier's constant, respectively.
[37] See Supplemental Material at http://link.aps.org/supplemental/10.1103/PhysRevLett.113.096403, which includes Refs. [38–42], for the details of the evaluation procedures of x_{ph}, the initial dynamics of ΔR, the analyses of the ε_2 spectra, the Raman-mode frequency calculation, the analyses of coherent oscillations on ΔR, and the nature of photoinduced Mott-insulator to CDW and Mott-insulator to metal transitions.
[38] H. Kishida, H. Matsuzaki, H. Okamoto, T. Manabe, M. Yamashita, Y. Taguchi, and Y. Tokura, Nature (London) **405**, 929 (2000).
[39] T. Ogasawara, M. Ashida, N. Motoyama, H. Eisaki, S. Uchida, Y. Tokura, H. Ghosh, A. Shukla, S. Mazumdar, and M. Kuwata-Gonokami, Phys. Rev. Lett. **85**, 2204 (2000).

[40] H. Kishida, M. Ono, K. Miura, H. Okamoto, M. Izumi, T. Manako, M. Kawasaki, Y. Taguchi, Y. Tokura, T. Tohyama, K. Tsutsui, and S. Maekawa, Phys. Rev. Lett. **87**, 177401 (2001).

[41] M. Ono, H. Kishida, and H. Okamoto, Phys. Rev. Lett. **95**, 087401 (2005).

[42] R. P. Feynman, Phys. Rev. **56**, 340 (1939).

[43] Before the KKT, ΔR data were interpolated. $(R + \Delta R)$ spectra were extrapolated assuming that R and ΔR values outside the measured regions were equal to those at the lower- or higher-energy bounds.

[44] First, the parameter values were assumed to be around those determined for another PdBr compound in the past: $U \sim 3$, $V \sim 1$, $S \sim 0.2$, and $t_0 \sim 1$ eV [35,45].

[45] H. Matsuzaki, K. Iwano, T. Aizawa, M. Ono, H. Kishida, M. Yamashita, and H. Okamoto, Phys. Rev. B **70**, 035204 (2004).

[46] In this analysis, we assumed a linear relation between t_0 and S, which gives the reasonable values of E_g.

[47] H. J. Zeiger, J. Vidal, T. K. Cheng, E. P. Ippen, G. Dresselhaus, and M. S. Dresselhaus, Phys. Rev. B **45**, 768 (1992).

[48] K. Kimura, H. Matsuzaki, S. Takaishi, M. Yamashita, and H. Okamoto, Phys. Rev. B **79**, 075116 (2009).